Brain (2002), **125,** 1358–1365

Striatal and extrastriatal dysfunction in Parkinson's disease with dementia: a 6-[^{18}F]fluoro-L-dopa PET study

Kengo Ito,[1] Atsuko Nagano-Saito,[1] Takashi Kato,[1] Yutaka Arahata,[1] Akinori Nakamura,[1] Yasuhiro Kawasumi,[1] Kentaro Hatano,[1] Yuji Abe,[2] Takako Yamada,[2] Teruhiko Kachi[2] and David J. Brooks[3,4]

[1]*Department of Biofunctional Research, National Institute for Longevity Sciences and* [2]*Department of Neurology, Chubu National Hospital, Obu, Japan,* [3]*MRC Clinical Sciences Centre, Imperial College School of Medicine, Hammersmith Hospital, London and* [4]*Institute of Neurology, Queen Square, London, UK*

Correspondence to: Dr Kengo Ito, Department of Biofunctional Research, National Institute for Longevity Sciences, 36-3 Gengo, Morioka-cho, Obu, Aichi Prefecture, 474-8522, Japan
E-mail: kito@nils.go.jp

Summary

We investigated the relative differences in dopaminergic function through the whole brain in patients with Parkinson's disease without dementia (PD) and with dementia (PDD) using 6-[^{18}F]fluoro-L-dopa (^{18}F-dopa) PET and a voxel-by-voxel analysis. The 10 PD and 10 PDD patients were equivalently disabled, having mean scores of 3.2 ± 0.6 and 3.2 ± 0.7, respectively, on the Hoehn and Yahr rating scale. ^{18}F-dopa influx constant (Ki) images of those patients and 15 normal age-matched subjects were transformed into standard stereotactic space. The significant differences between the groups (expressed in mean regional Ki values) were localized with statistical parametric mapping (SPM) on a voxel-by-voxel basis. Compared with the normal group, SPM localized declines of the ^{18}F-dopa Ki bilaterally in the putamen, the right caudate nucleus and the left ventral midbrain for the PD group ($P < 0.01$, corrected). Compared with the normal group, the PDD group showed reduced ^{18}F-dopa Ki bilaterally in the striatum, midbrain and anterior cingulate area ($P < 0.01$, corrected). A relative difference in ^{18}F-dopa uptake between PD and PDD was the bilateral decline in the anterior cingulate area and ventral striatum and in the right caudate nucleus in the PDD group ($P < 0.001$, corrected). Accordingly, we conclude that dementia in PD is associated with impaired mesolimbic and caudate dopaminergic function.

Keywords: 6-[^{18}F]fluoro-L-dopa; positron emission tomography; Parkinson's disease; Parkinson's disease with dementia

Abbreviations: AADC = aromatic aminoacid decarboxylase; DLB = dementia with Lewy bodies; Ki = ^{18}F-dopa influx constant; PD = Parkinson's disease without dementia; PDD = Parkinson's disease with dementia; ROI = region of interest; SN = substantia nigra; SPM = statistical parametric mapping; UPDRS = unified Parkinson's disease rating scale; VTA = ventral tegmental area

Introduction

The use of 6-[^{18}F]fluoro-L-dopa (^{18}F-dopa) with PET permits the study of presynaptic dopaminergic terminal function in the striatum *in vivo* in both healthy volunteers and Parkinson's disease (PD) patients. In PD, this technique has been used to provide a measure of disease severity and to identify individuals with early, and even preclinical, disease (Garnett *et al*., 1987; Bhatt *et al*., 1991; Brooks *et al*., 1991; Burn *et al*., 1992; Sawle *et al*., 1992; Morrish *et al*., 1995).

Although the main dopaminergic projections are nigrostriatal, extrastriatal dopamine terminals are also involved to varying extents in different phenotypes of idiopathic PD and other parkinsonian syndromes. Already, previous studies have reported the association between cognitive impairment and dopaminegic dysfunction in PD using ^{18}F-dopa PET and conventional region of interest (ROI) analysis (Holthoff-Detto *et al*., 1997; Rinne *et al*., 2000). However, accurate detection of dopaminergic changes in cortical and brainstem areas, where ^{18}F-dopa uptake constants are lower than those in the striatum, is unreliable using conventional ROI analysis, as an *a priori* judgement must be made about region size and

© *Guarantors of Brain 2002*

Table 1 *Clinical characteristics of patients and control groups*

Characteristics	Normal controls (n = 15)	Patients with Parkinson's disease	
		PD (n = 10)	PDD (n = 10)
Age (years)	67.4 ± 5.2	65.8 ± 6.7	66.1 ± 6.9
Sex (M/F)	4/11	2/8	7/3
Disease duration (years)	NA	6.6 ± 4.7	8.1 ± 6.0
Hoehn and Yahr rating score	NA	3.2 ± 0.6	3.2 ± 0.7
Motor UPDRS	NA	36.1 ± 16.1*	37.4 ± 12.8†
MMSE	29.2 ± 1.1	27.9 ± 2.2	20.4 ± 4.7‡

NA = not applicable; *n = 8; †n = 7; ‡$P < 0.001$ versus without dementia.

placement over potential sites of loss of dopaminergic function. As a consequence, the ROI approach is not suited for use as an exploratory technique with ^{18}F-dopa PET. Thus, we developed a technique for spatially normalizing ^{18}F-dopa influx (Ki) images, and have used statistical parametric mapping (SPM) to assess the extrastriatal uptake of ^{18}F-dopa in normal and PD brains (Ito *et al*., 1999; Rakshi *et al*., 1999; Nagano *et al*., 2000).

In this study, we applied our normalization and SPM approach to equivalently disabled Parkinson's disease patients without (PD) and with (PDD) dementia in order to localize relative differences in their pathophysiologies on a voxel-by-voxel basis.

Material and methods

Subjects

Ten patients with idiopathic PD (six right dominant and four left dominant; mean age 65.8 ± 6.7 years) without dementia and 10 patients with PDD (seven right dominant and three left dominant; mean age 66.1 ± 6.9 years) were recruited from the Chubu National Hospital Neurology Clinic. All PD patients fulfilled UK Brain Bank criteria for diagnosis of this disorder. The PDD patients met the criteria for PDD, namely parkinsonism plus dementia, where the motor manifestations preceded the cognitive ones by at least 1 year (McKeith *et al*., 1996). Although the PDD patients included some cases with a relatively high mini mental state examination (MMSE) score, all fulfilled Diagnostic and Statistical Manual (DSM) IV criteria for dementia. The 10 PD and 10 PDD patients were equivalently disabled, having a mean score of 3.2 ± 0.6 and 3.2 ± 0.7, respectively, on the Hoehn and Yahr rating scale. Motor unified Parkinson's disease rating scale (UPDRS) score was available for eight PD and seven PDD patients, and there was no significant difference between two groups. The PD and PDD patients without significant cerebral atrophy beyond what would be expected for age on MRI were selected for PET in order to minimize partial volume effects due to brain volume loss. Each patient was assessed clinically by neurologists before PET and at least 48 h after discontinuing their medications. The PDD patients in this study were given no specific treatment, such as acetylcholinesterase inhibitors, for their dementia. Details of the patients are shown in Table 1.

A separate group of 15 normal volunteers (mean age 67.4 ± 5.2 years) was recruited and scanned over the same time period. These 15 volunteers had no symptoms or signs suggestive of a neurological disorder and displayed no significant structural abnormalities except for normal age-related changes, such as dilated perivascular spaces, on their MRIs.

Permission to perform this study was obtained from the Ethical Committee of the Chubu National Hospital. All of the subjects gave written informed consents prior to PET scanning.

PET study

An oral bolus (100 mg) of carbidopa, a peripheral aromatic amino acid decarboxylase inhibitor, was given 1 h before scanning. Dynamic ^{18}F-dopa PET studies were performed using an ECAT EXACT HR47 (CTI/Siemens, Knoxville, Tenn., USA) in three-dimensional acquisition mode, which yielded 47 simultaneous planes, with an axial full-width half-maximum (FWMH) resolution of 4.8 mm and an in-plane resolution of 3.9 × 3.9 mm. An air cushion was inflated such that it moulded to the shape of the back of the head of each subject, thus minimizing head movements. Correction for tissue attenuation of 511 keV γ radiation was measured with a 10 min, two-dimensional transmission scan performed prior to the tracer injection using three retractable ^{68}Ga/^{68}Ge sources.

Eighty to 180 MBq of ^{18}F-dopa were infused intravenously into each subject over 30 s. Scanning began at the start of tracer injection. The protocol included 25 time frames (4 × 1 min, 3 × 2 min, 3 × 3 min, 15 × 5 min) over 94 min.

All of the subjects underwent high-resolution volumetric MRI with a Visart 1.5 T MRI (Toshiba, Tokyo, Japan). A field echo sequence protocol (TR: 20 ms; TE: 7 ms; flip angle: 35°) generated 1.5-mm thick sagittal images without slice gaps.

Functional mapping and spatial normalization of images

Data analysis was performed on a Sun workstation (Sun Microsystems, Silicon Valley, Calif., USA). In order to correct for head movement during scans, a dynamic file from each subject was divided into time frames and then each time frame was aligned to the mean image of all frames using the alignment program in SPM95.

The ^{18}F-dopa influx constant (Ki) image and integrated 'add image' were created using 'kronos' software developed by D. Bailey (MRC Cyclotron Unit, Hammersmith Hospital, London, UK) and implemented in IDL Image Analysis software (Research Systems, Inc., Boulder, Col., USA), based on the multiple time graphical analysis (MTGA) approach of Patlak and Blasberg (Patlak *et al*., 1983, 1985). The 'add image' comprised integrated 30–94 min time frames of the ^{18}F-dopa dynamic images. We used the cerebellar tissue counts between 0 and 94 min post-injection as a reference tissue input function, and brain tissue activity on a voxel-by-voxel basis between 30 and 94 min to compute the gradient of the linear regression line representing Ki with the MTGA approach. The right and left cerebellar ROIs defining the input function were placed on each of three contiguous slices.

Using ANALYZE 7.0 software (Mayo Foundation, Baltimore, Md., USA), the scalp was edited from the MRI and the ^{18}F-dopa add image of each subject. The ^{18}F-dopa add image was then co-registered to each individual MRI using Automated Image Registration (AIR) software developed by Woods (Woods *et al*., 1992, 1993). The Ki image was also co-registered to each individual MR image, using the same parameters as those used to co-register the respective ^{18}F-dopa add image to the MRIs.

The MRIs were transformed into standard stereotactic space of Talairach and Tournoux (Talairach *et al*., 1988) using the normalization program in SPM95. We developed our normalization technique for ^{18}F-dopa images with SPM95 (Nagano *et al*., 2000). Therefore, the MRI template provided in SPM95 was used for this normalization. The co-registered ^{18}F-dopa Ki images were then transformed into standard stereotactic space using the parameters of spatial normalization applied to the MRIs of each subject.

Statistical parametric mapping

Significant differences in mean regional Ki values between different groups were localized with SPM96 (Wellcome Department of Cognitive Neurology, London, UK) on a voxel-by-voxel basis. A Gaussian kernel of $8 \times 8 \times 8$ mm (FWHM in the x, y and z planes, respectively) was applied to remove high-frequency noise from the images. Appropriate contrasts were used to derive the (unpaired) t statistic between the groups using the general linear model. The resulting set of voxel t values constitutes an SPM$\{t\}$, which is used to make inferences about regionally significant changes in Ki (Friston *et al*., 1991). The SPM$\{t\}$s were transformed to maps of Z scores (SPM$\{Z\}$) for display purposes. The P values associated with regional differences in Ki were corrected for multiple dependent comparisons implicit in SPM96 using the theory of Gaussian fields. Maps of Z scores surviving a threshold of 2.33 ($P < 0.01$) and extent corrected $P < 0.05$ were generated to detect significant differences between patients and healthy controls. In contrast, for the comparison between the PD and PDD patients, maps of Z scores surviving a more conservative threshold of 3.09 ($P < 0.001$) and extent corrected $P < 0.05$ were applied.

ROI analysis

In order to calculate the mean value and standard deviation of Ki corresponding to each significant area on SPM$\{Z\}$, an ROI analysis was performed. As we previously reported, the automated ROI analysis was applicable to spatially normalized Ki images of ^{18}F-dopa across different cases, and its result was identical to conventional ROI analysis (Ito *et al*., 1999; Nagano *et al*., 2000). Therefore, ROIs were drawn on the MRI template in SPM95 and transferred to the spatially normalized Ki images. Considering the known dopaminergic projections in the human brain and the results of group comparison between PDD and normal controls with SPM, ROIs were defined for the caudate, putamen, ventral midbrain, amygdala, hippocampus and anterior cingulate cortex on each of three contiguous planes. The ROIs depicted on the templates were applied to each of the three adjacent planes of spatially normalized Ki images of each subject and mean regional Ki values were calculated for each individual. The mean regional Ki values between the groups were compared by analysis of variance (ANOVA) and *post hoc* Fisher's PLSD (protected least significant difference) to correct for multiple comparisons.

Results

SPM localized a significant reduction in mean ^{18}F-dopa Ki in the putamen bilaterally, right caudate nucleus and left ventral midbrain for the PD group compared with the normal controls ($P < 0.01$, corrected). The mean Ki of left caudate nucleus was also decreased, but the reduction failed to reach statistical significance ($P < 0.05$, corrected). Compared with the normal group, the PDD patients showed significant declines in ^{18}F-dopa uptake bilaterally in the caudate nucleus, putamen, midbrain and anterior cingulate area ($P < 0.01$, corrected). The corresponding SPMs and peak coordinates in SPM analysis are shown in Fig. 1 and Table 2. Compared with the PD group, the PDD patients showed consistent declines in ^{18}F-dopa Ki bilaterally in the anterior cingulate area 32 and ventral striatum and in the right caudate nucleus ($P < 0.001$, corrected). There were also similar trends bilaterally in the putamen and in the left caudate nucleus, but these did not reach statistical significance ($P < 0.05$, corrected). The declines in the ^{18}F-dopa Ki for the left amygdala also failed to reach statistical significance ($P < 0.01$, corrected). The

corresponding SPMs and peak coordinates in SPM analysis between PD and PDD are shown in Fig. 2 and Table 2. No significant increases in Ki were observed for either PD or PDD patients compared with the normal group.

The results of Ki measurements from the ROI analysis are shown in Fig. 3 and Table 3. Compared with the normal group, the PDD patients showed significant declines in ^{18}F-dopa Ki bilaterally in the caudate nucleus, putamen, ventral midbrain and anterior cingulate area. Compared with the PD group, the mean Ki values in the PDD group were further decreased in all regions and the reductions reached statistical significance in the caudate nucleus and putamen bilaterally, as well as in the left anterior cingulate area and left amygdala. There was also a similar trend in the right anterior cingulate area, although it was not statistically significant.

In order to clarify a statistical correlation between ^{18}F-dopa uptake and MMSE, significant correlations were localized with SPM96 on a voxel-by-voxel basis in 20 patients (both PD and PDD subjects). The MMSE score significantly correlated with the Ki values in the right caudate nucleus ($P < 0.001$, corrected). There were also similar trends bilaterally in the putamen, ventral striatum, anterior cingulate area and hippocampus, but these did not reach statistical significance ($P < 0.01$, corrected). The corresponding SPMs are shown in Fig. 4.

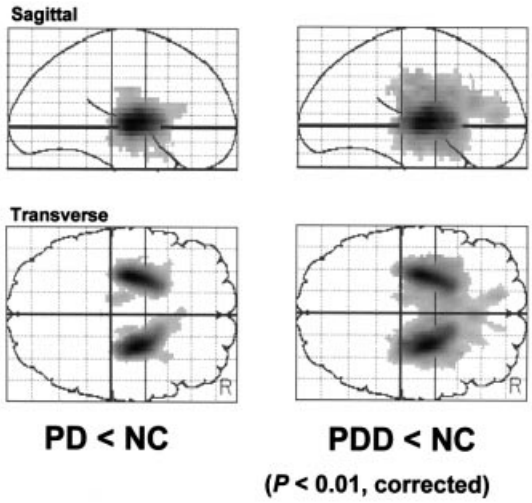

Fig. 1 SPMs showing the spatial distribution of significant regions ($P < 0.01$, corrected) where Ki decreased in PD (*left*) and PDD (*right*) compared with the normal control (NC). Images are shown as integrated projections along sagittal and transverse views of the Talairach and Tournoux brain atlas.

Discussion

Concomitant dementia represents a significant clinical problem in Parkinson's disease patients, its prevalence being estimated to be ~20% of all PD patients (Lieberman *et al*., 1979; Brown *et al*., 1984). Pathologically, dementia in Parkinson's disease has been attributed to direct involvement of the cortex by Lewy body (LB) pathology (Kosaka *et al*., 1984, 1993), incidental Alzheimer's disease (Hakim *et al*., 1979; Boller *et al*., 1980), loss of cholinergic projections due to degeneration of the basal nucleus of Meynert (Whitehouse *et al*., 1983; Gaspar *et al*., 1984) and loss of mesolimbic and mesocortical dopaminergic projections due to degeneration of medial substantia nigra (SN) and ventral tegmental area (VTA) (Torack *et al*., 1988; Rinne *et al*., 1989). A previous clinicopathological study has reported that among 44 patients

Table 2 *Peak coordinates in SPM analysis*

P (corrected)	^{18}F-dopa Ki	Region	Coordinates (mm)			*Z* score
			x	*y*	*z*	
Comparison of PD with normal group						
0.000	1700	Rt caudate and putamen	24	–6	4	8.44
0.000	1536	Lt putamen	–26	–12	4	8.45
		Lt ventral midbrain	–12	–16	–12	3.38
Comparison of PDD with normal group						
0.000	7633	Rt caudate and putamen	24	–6	4	9.20
		Lt caudate and putamen	–26	–12	4	8.89
		Rt ventral midbrain	16	–18	–12	4.64
		Lt ventral midbrain	–10	–16	–12	3.59
		Rt ant cingulate	2	26	16	4.26
		Lt ant cingulate	–10	44	8	3.77
Comparison of PDD with PD						
0.000	181	Rt ventral striatum	16	4	–12	4.91
0.000	268	Rt caudate	16	4	8	4.36
0.000	210	Lt ventral striatum	–18	14	–12	4.62
		Rt ant cingulate	4	26	–8	3.99
		Lt ant cingulate	–8	44	12	5.02

Maximum peak coordinate for each anatomical region is listed. Rt, right; Lt, left; ant, anterior.

with PDD, 29% had Alzheimer's disease, 10% had numerous cortical LBs, 6% had a possible vascular cause and in 55% no definite pathologic cause was found. Owing to such heterogeneity in mechanisms of dementia in PD, the relationship of PDD to PD and to dementia with LBs (DLB) still requires clarification (Perry *et al*., 1990; Mega *et al*., 1996). Functional imaging with PET provides an objective means of revealing the pathophysiology of neurodegenerative diseases and supplements clinical diagnosis. Specifically, we have used PET to assess dopaminergic function, which is impaired in PDD and PD, in order to reveal their pathophysiology.

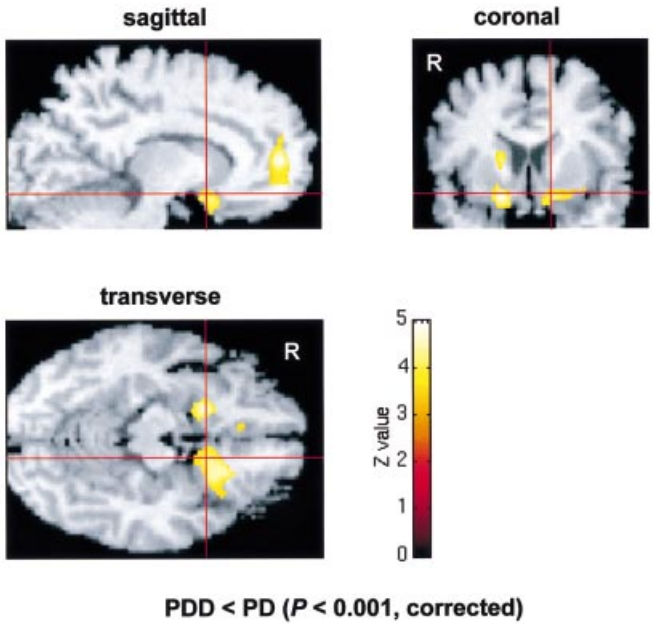

Fig. 2 Significant regions ($P < 0.001$, corrected) of decreased dopamine metabolism (Ki) in PDD compared with PD superimposed on a normalized brain MRI. SPM showed relative declines of ^{18}F-dopa uptake bilaterally in the anterior cingulate area and ventral striatum and in the right caudate nucleus.

With SPM, we found that the PDD group showed additional significant reductions in ^{18}F-dopa uptake in voxels distributed over the anterior cingulate area, ventral striatum bilaterally and the right caudate nucleus compared with non-demented PD patients. These findings are in line with *post mortem* studies that have demonstrated severe involvement of the mesolimbic and mesocortical dopaminergic system in addition to the nigrostriatal system in PDD patients (Rinne *et al*., 1989). Mesolimbic dopamine projections, including those to the anterior cingulate area and ventral striatum, originate from cell bodies in the medial SN and midbrain VTA. Therefore, this study reinforces our view that dementia in PD is associated with involvement of the medial part of the SN and VTA.

The MMSE score in the combined group of PD and PDD patients significantly correlated with the Ki values in the right caudate nucleus; there were also similar trends bilaterally in the putamen, ventral striatum, anterior cingulate area and hippocampus. Correspondingly, the association between the degree of cognitive impairment and ^{18}F-dopa uptake in the caudate nucleus and medial frontal cortex has been reported in PD patients via PET (Holthoff-Detto *et al*., 1997; Rinne *et al*., 2000). In addition, the correlation between the orbitofrontal binding site density of dopamine transporter and mentation scores of the UPDRS in early PD has been reported (Ouchi *et al*., 1999), as has the correlation between the right caudate binding site density of dopamine transporter and frontal executive performance (Marie *et al*., 1999). These findings suggest that caudate, mesolimbic and mesocortical dopaminergic dysfunction plays an important role in the cognitive impairment of PD. There may also be an additional association with temporo-parietal dysfunction, as FDG PET

Table 3 *Mean regional Ki values in normal, PD and PDD*

	Ki/min											
	Rt caudate	Lt caudate	Rt putamen	Lt putamen	Rt ventral midbrain	Lt ventral midbrain	Rt ant cingulate	Lt ant cingulate	Rt amygdala	Lt amygdala	Rt hippo-campus	Lt hippo-campus
Normal (n =15)												
Mean	0.0092	0.0086	0.0093	0.0092	0.0027	0.0029	0.0016	0.0016	0.0037	0.0034	0.0023	0.0024
SD	0.0011	0.0011	0.0010	0.0012	0.0008	0.0010	0.0004	0.0006	0.0004	0.0009	0.0004	0.0004
PD (n = 10)												
Mean	0.0069	0.0070	0.0042	0.0042	0.0022	0.0021	0.0015	0.0016	0.0035	0.0038	0.0025	0.0024
SD	0.0012	0.0014	0.0009	0.0008	0.0007	0.0005	0.0006	0.0005	0.0005	0.0009	0.0005	0.0005
P values*	0.002	0.008	<0.001	<0.001	n.s.	0.023	n.s.	n.s.	n.s.	n.s.	n.s.	n.s.
PDD (n = 10)												
Mean	0.0051	0.0056	0.0031	0.0032	0.0017	0.0017	0.0011	0.0011	0.0032	0.0027	0.0020	0.0023
SD	0.0016	0.0016	0.0011	0.0008	0.0005	0.0004	0.0003	0.0003	0.0009	0.0008	0.0006	0.0008
P values*	<0.001	<0.001	<0.001	<0.001	0.003	0.001	0.031	0.021	n.s.	n.s.	n.s.	n.s.
P values†	0.008	0.021	0.029	0.045	n.s.	n.s.	n.s.	0.044	n.s.	0.019	n.s.	n.s.

*Comparison of PD or PDD with normal group; †comparison of PDD with PD. Lt, left; Rt, right; n.s., not significant.

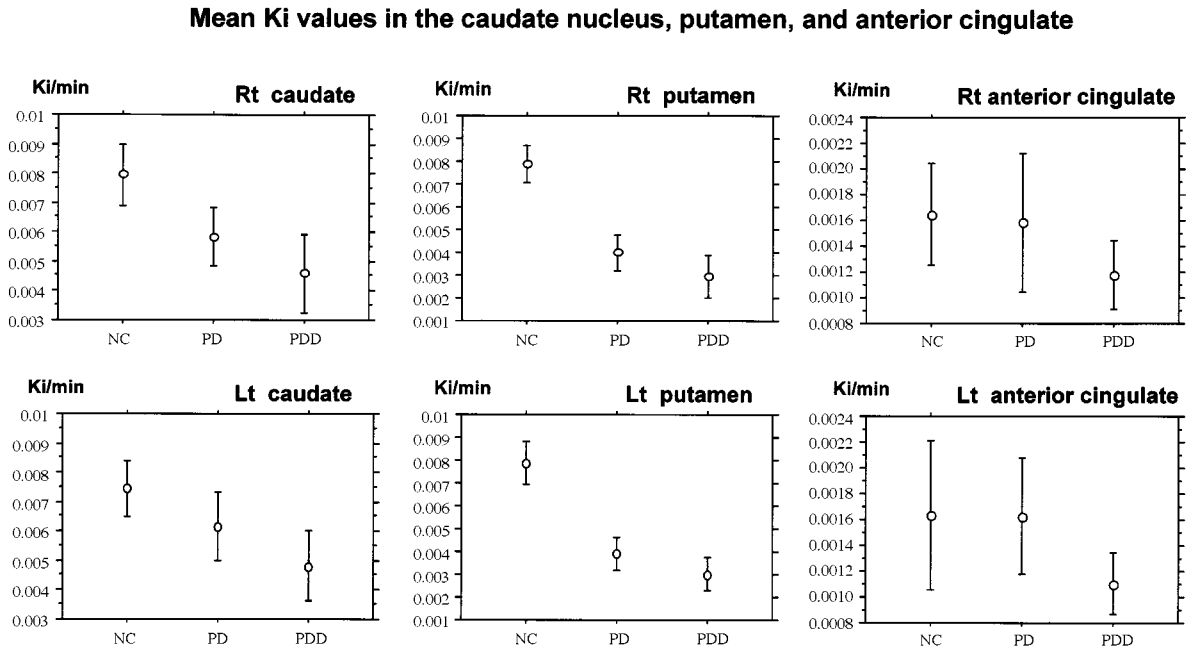

Fig. 3 The mean Ki values in the caudate nucleus, putamen and anterior cingulate area for the normal control (NC), PD and PDD patients in the ROI analysis. Bars are standard deviations. The mean Ki value in the anterior cingulate area decreased only for PDD compared with normal control. In contrast to this, the mean Ki values in the caudate nucleus and putamen decreased for both PD and PDD.

has shown glucose hypometabolism in these areas in PDD (Schapiro *et al*., 1993; Vander *et al*., 1997).

The anterior cingulate is within the areas that show the most obvious pathological changes in DLB and PDD (Pellise *et al*., 1996). Furthermore, atrophy of the cingulate cortex has been noted pathologically in PD (Braak *et al*., 1995). For this reason, our cases of PD and PDD were carefully selected to have non-atrophic MRIs, in order to minimize any partial volume effects. Although the potential cortical pathology could be a potential explanation for reduced ^{18}F-dopa uptake in the anterior cingulate, our results suggest that demented PD patients have reduced cingulate aromatic amino-acid decarboxylase (AADC) activity before focal cerebral atrophy can be detected.

There were a few differences in statistical significance between SPM and the automated ROI analysis. We believe that these differences probably arose as a result of the different statistical approaches used in the two analyses. SPM is performed on a voxel basis and uses the general linear model and the theory of continuous random fields to correct for multiple comparisons, while Kis from ROIs were interrogated with ANOVA and *post hoc* Fisher's PLSD.

Previously, we reported an increased Ki in early PD and an unchanged Ki in advanced PD in the cingulate cortex compared with normal controls (Rakshi *et al*., 1999). In this study, the Ki in the cingulate cortex did not show any significant change in the PD group compared with the normal group. These results are considered to be compatible with our previous report, because the PD group in this study consisted of established PD cases with a mean score of 3.2 ± 0.6 on the Hoehn and Yahr rating scale.

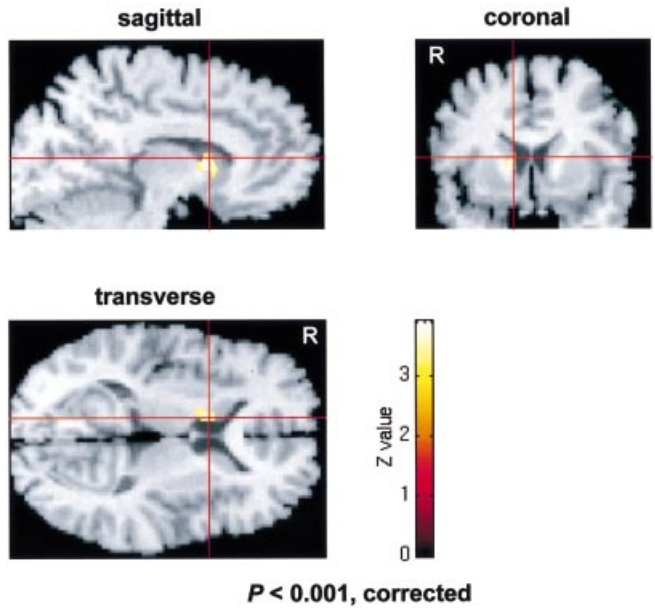

Fig. 4 Significant regions ($P < 0.001$, corrected) of correlation between ^{18}F-dopa uptake and MMSE in the combined group of PD and PDD patients, superimposed on a normalized brain MRI. The MMSE score positively correlated with the Ki values in the right caudate nucleus.

^{18}F-dopa is decarboxylated by AADC to yield ^{18}F-dopamine (Tison *et al*., 1991). Therefore, the Ki value is considered to be an index of AADC activity. The normal subjects had relatively high Ki values within the midbrain, amygdala, hippocampus and cingulate cortex, as well as in

the caudate nucleus and putamen. These regions all correspond to dopaminergic projection areas in the brain; however, recent studies have suggested that noradrenergic and serotoninergic neurones also display AADC activity (Arai *et al*., 1996). Accordingly, the findings in our study could also reflect possible impairments of the noradrenergic and serotoninergic projections. Despite this possibility, we believe that the non-selectivity of ^{18}F-dopa is not a disadvantage, but allows sensitive detection of monoaminergic dysfunction.

So far, the function of pre- and postsynaptic cholinergic termini has been evaluated in Parkinson's disease using [^{123}I]iodobenzovesamicol (IBVM) single photon emission computed tomography (SPECT) (Kuhl *et al*., 1996) and ^{11}C-*N*-methyl-4-piperidyl benzilate (NMPB) PET (Asahina *et al*., 1998), respectively. These studies have suggested that cholinergic dysfunction might contribute to the cognitive impairment observed in Parkinson's disease. Therefore, to clarify the relation between dopaminergic and cholinergic dysfunction in Parkinson's disease, further comparative investigation is required.

This study demonstrates the impairment of striatal and extrastriatal function *in vivo* in PDD. The application of SPM to ^{18}F-dopa PET enables objective localization of impairments in monoaminergic function throughout the brain at a voxel level, and allows for comparisons of the regional differences in monoaminergic metabolism between PD and related disorders, including DLB. We believe that loss of mesolimbic and mesocortical dopaminergic projections is also likely to play an important role in the pathophysiology of DLB, which is included within the spectrum of Lewy body disease as well as PD and PDD.

Conclusion

In this study we have demonstrated a significant dysfunction in both the striatal and extrastriatal regions in PD patients with super-added dementia. These findings are consistent with the hypothesis that impairment of mesolimbic and caudate dopaminergic function plays an important role in the dementia of PD.

Acknowledgements

This study was supported by the fund for Comprehensive Research of Aging and Health and the fund for Brain Science from the Ministry of Welfare, Japan.

References

Arai R, Karasawa N, Nagatsu I. Aromatic L-amino acid decarboxylase is present in serotonergic fibers of the striatum of the rat. A double-labeling immunofluorescence study. Brain Res 1996; 706: 177–9.

Asahina M, Suhara T, Shinotoh H, Inoue O, Suzuki K, Hattori T. Brain muscarinic receptors in progressive supranuclear palsy and Parkinson's disease: a positron emission tomographic study. J Neurol Neurosurg Psychiatry1998; 65: 155–63.

Bhatt MH, Snow BJ, Martin WR, Pate BD, Ruth TJ, Calne DB. Positron emission tomography suggests that the rate of progression of idiopathic parkinsonism is slow. Ann Neurol 1991; 29: 673–7.

Boller F, Mizutani T, Roessmann U, Gambetti P. Parkinson disease, dementia, and Alzheimer disease: clinicopathological correlations. Ann Neurol 1980; 7: 329–35.

Braak H, Braak E, Yilmazer D, Schultz C, de Vos RA, Jansen EN. Nigral and extranigral pathology in Parkinson's disease. [Review]. J Neural Transm Suppl 1995; 46: 15–31.

Brooks DJ. Detection of preclinical Parkinson's disease with PET. Neurology 1991; 41 (5 Suppl 2): 24–7.

Brown RG, Marsden CD. How common is dementia in Parkinson's disease? Lancet 1984; 2: 1262–5.

Burn DJ, Mark MH, Playford ED, Maraganore DM, Zimmerman TR, Duvoisin RC, et al. Parkinson's disease in twins studied with ^{18}F-dopa and positron emission tomography. Neurology 1992; 42: 1894–900.

Friston KJ, Frith CD, Liddle PF, Frackowiak RS. Comparing functional (PET) images: the assessment of significant change. J Cereb Blood Flow Metab 1991; 11: 690–9.

Garnett ES, Lang AE, Chirakal R, Firnau G, Nahmias C. A rostrocaudal gradient for aromatic acid decarboxylase in the human striatum. Can J Neurol Sci 1987; 14 (3 Suppl): 444–7.

Gaspar P, Gray F. Dementia in idiopathic Parkinson's disease. A neuropathological study of 32 cases. Acta Neuropathol (Berl) 1984; 64: 43–52.

Hakim AM, Mathieson G. Dementia in Parkinson disease: a neuropathologic study. Neurology 1979; 29: 1209–14.

Holthoff-Detto VA, Kessler J, Herholz K, Bonner H, Pietrzyk U, Wurker M, et al. Functional effects of striatal dysfunction in Parkinson disease. Arch Neurol 1997; 54: 145–50.

Ito K, Morrish PK, Rakshi JS, Uema T, Ashburner J, Bailey DL, et al. Statistical parametric mapping with 18F-dopa PET shows bilaterally reduced striatal and nigral dopaminergic function in early Parkinson's disease. J Neurol Neurosurg Psychiatry 1999; 66: 754–8.

Kosaka K. Dementia and neuropathology in Lewy body disease. Adv Neurol 1993; 60: 456–63.

Kosaka K, Yoshimura M, Ikeda K, Budka H. Diffuse type of Lewy body disease: progressive dementia with abundant cortical Lewy bodies and senile changes of varying degree—a new disease? Clin Neuropathol 1984; 3: 185–92.

Kuhl DE, Minoshima S, Fessler JA, Frey KA, Foster NL, Ficaro EP, et al. In vivo mapping of cholinergic terminals in normal aging, Alzheimer's disease, and Parkinson's disease. Ann Neurol 1996; 40: 399–410.

Lieberman A, Dziatolowski M, Kupersmith M, Serby M, Goodgold A, Korein J, et al. Dementia in Parkinson disease. Ann Neurol 1979; 6: 355–9.

Marie RM, Barre L, Dupuy B, Viader F, Defer G, Baron JC.

Relationships between striatal dopamine denervation and frontal executive tests in Parkinson's disease. Neurosci Lett 1999; 260: 77–80.

McKeith IG, Galasko D, Kosaka K, Perry EK, Dickson DW, Hansen LA, et al. Consensus guidelines for the clinical and pathologic diagnosis of dementia with Lewy bodies (DLB): report of the consortium on DLB international workshop. [Review]. Neurology 1996; 47: 1113–24.

Mega MS, Masterman DL, Benson DF, Vinters HV, Tomiyasu U, Craig AH, et al. Dementia with Lewy bodies: reliability and validity of clinical and pathologic criteria. Neurology 1996; 47: 1403–9.

Morrish PK, Sawle GV, Brooks DJ. Clinical and [^{18}F] dopa PET findings in early Parkinson's disease. J Neurol Neurosurg Psychiatry 1995; 59: 597–600.

Nagano AS, Ito K, Kato T, Arahata Y, Kachi T, Hatano K, et al. Extrastriatal mean regional uptake of fluorine-18-FDOPA in the normal aged brain – an approach using MRI-aided spatial normalization. Neuroimage 2000; 11: 760–6.

Ouchi Y, Yoshikawa E, Okada H, Futatsubashi M, Sekine Y, Iyo M, et al. Alterations in binding site density of dopamine transporter in the striatum, orbitofrontal cortex, and amygdala in early Parkinson's disease: compartment analysis for beta-CFT binding with positron emission tomography. Ann Neurol 1999; 45: 601–10.

Patlak CS, Blasberg RG. Graphical evaluation of blood-to-brain transfer constants from multiple-time uptake data. Generalizations. J Cereb Blood Flow Metab 1985; 5: 584–90.

Patlak CS, Blasberg RG, Fenstermacher JD. Graphical evaluation of blood-to-brain transfer constants from multiple-time uptake data. J Cereb Blood Flow Metab 1983; 3: 1–7.

Pellise A, Roig C, Barraquer-Bordas LI, Ferrer I. Abnormal, ubiquitinated cortical neurites in patients with diffuse Lewy body disease. Neurosci Lett 1996; 206: 85–8.

Perry PH, Irving D, Blessed G, Fairbairn A, Perry EK. Senile dementia of Lewy body type. J Neurol Sci 1990; 95: 119–39.

Rakshi JS, Uema T, Ito K, Bailey DL, Morrish PK, Ashburner J, et al. Frontal, midbrain and striatal dopaminergic function in early and advanced Parkinson's disease. A 3D [^{18}F]dopa-PET study. Brain 1999; 122: 1637–50.

Rinne JO, Rummukainen J, Paljarvi L, Rinne UK. Dementia in Parkinson's disease is related to neuronal loss in the medial substantia nigra. Ann Neurol 1989; 26: 47–50.

Rinne JO, Portin R, Ruottinen H, Nurmi E, Bergman J, Haaparanta M, et al. Cognitive impairment and the brain dopaminergic system in Parkinson disease: [^{18}F]fluorodopa positron emission tomographic study. Arch Neurol 2000; 57: 470–5.

Sawle GV, Wroe SJ, Lees AJ, Brooks DJ, Frackowiak RS. The identification of presymptomatic parkinsonism; clinical and ^{18}F-dopa positron emission tomography studies in an Irish kindred. Ann Neurol 1992; 32: 609–17.

Schapiro MB, Pietrini P, Grady CL, Ball MJ, DeCarli C, Kumar A, et al. Reductions in parietal and temporal cerebral metabolic rates for glucose are not specific for Alzheimer's disease. J Neurol Neurosurg Psychiatry 1993; 56: 859–64.

Talairach J, Tournoux P. Co-planar stereotaxic atlas of the human brain. Stuttgart: Thieme; 1988.

Tison F, Normand E, Jaber M, Aubert I, Bloch B. Aromatic L-amino-acid decarboxylase (DOPA decarboxylase) gene expression in dopaminergic and serotoninergic cells of the rat brainstem. Neurosci Lett 1991; 127: 203–6.

Torack RM, Morris JC. The association of ventral tegmental area histopathology with adult dementia. Arch Neurol 1988; 45: 497–501.

VanderBorght T, Minoshima S, Giordani B, Foster NL, Frey KA, Berent S, et al. Cerebral metabolic differences in Parkinson's and Alzheimer's diseases matched for dementia severity. J Nucl Med 1997; 38: 797–802.

Whitehouse PJ, Hedreen JC, White CL 3rd, Price DL. Basal forebrain neurons in the dementia of Parkinson disease. Ann Neurol 1983; 13: 243–8.

Woods RP, Cherry SR, Mazziotta JC. Rapid automated algorithm for aligning and reslicing PET images. J Comput Assist Tomogr 1992; 16: 620–33.

Woods RP, Mazziotta JC, Cherry SR. MRI-PET registration with automated algorithm. J Comput Assist Tomogr 1993; 17: 536–46.

Received May 14, 2001. Revised November 23, 2001.
Second revision January 17, 2002. Accepted January 24, 2002